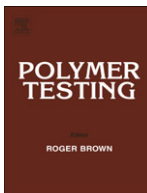




ELSEVIER

Contents lists available at SciVerse ScienceDirect

Polymer Testing

journal homepage: www.elsevier.com/locate/polytest

Material behaviour

Non-isothermal crystallization kinetics of recycled PET-Si₃N₄ nanocomposites

Wentao Hao^{a,*}, Xiaoming Wang^a, Wen Yang^a, Kang Zheng^b^a College of Chemical Engineering, Anhui Key Laboratory of Controllable Chemistry Reaction and Material Chemical Engineering, Hefei University of Technology, Hefei 230009, PR China^b Key Laboratory of Materials Physics, Institute of Solid State Physics, Chinese Academy of Sciences, Hefei 230031, PR China

ARTICLE INFO

Article history:

Received 22 August 2011

Accepted 8 October 2011

Keywords:

PET

Si₃N₄

Non-isothermal crystallization

Kinetics

ABSTRACT

Poly(ethylene terephthalate) (PET) is an important industrial material and has been widely applied in consumer products. Due to its slow crystallization rate, nanoparticles are incorporated into PET to function as heterogeneous nucleating agents. In this study, the non-isothermal crystallization behavior of recycled PET-silicon nitride (Si₃N₄) nanocomposites was investigated by differential scanning calorimetry (DSC). In the general analysis of the non-isothermal crystallization curves, it was found that the Si₃N₄ nanoparticles could effectively accelerate the nucleation of PET, but the crystal growth rate was slowed down when the Si₃N₄ content was more than 1 wt%. This might be attributed to the interaction between the PET chains and the surface-treated Si₃N₄ nanoparticles. Results obtained from Avrami and Mo treatments agreed well with the general analysis. Application of the Kissinger method and isoconversional method of Flynn-Wall-Ozawa also showed that Si₃N₄ nanoparticles had a good nucleation effect on the crystallization of PET, and the crystal growth was hindered by Si₃N₄ when the particle loading is higher than 1 wt%.

© 2011 Elsevier Ltd. All rights reserved.

1. Introduction

Polyethylene terephthalate (PET) is an important industrial material and is one of the commonly used polymer materials in consumer products. It can be made into drinking water bottles [1], optical films [2], ultra-fine fibers [3] etc. Due to its high melting temperature and low crystallization rate, PET is not suitable for high-speed processing, such as injection molding [4,5]. To enhance the overall crystallization ability of PET and to improve its mechanical performance, lots of work has been done on PET composites with different nanoparticles, including organic clay [6–8], SiO₂ [9–11], BaSO₄ [12,13] etc. However, there are not many reports on the crystallization behavior of the composites composed of recycled PET and nanoparticles [4,14]. Furthermore, to our best knowledge, there

is no scientific paper published on the non-isothermal crystallization kinetics of recycled PET-nanosized silicon nitride (Si₃N₄) composites.

Si₃N₄ is a type of ceramic material [15], and has not been widely applied in modification of polymer materials [16,17]. However, Si₃N₄ nanoparticles show unique influences on the crystallization behavior of isotactic polypropylene (iPP) [18,19]. It is our purpose in this study to further explore the influences of Si₃N₄ nanoparticles on the crystallization of PET, a polymer material totally different from iPP both in molecular structure and molecular motion.

2. Experiments

2.1. Materials

PET materials used in this study were cracked fragments of the pure water bottles produced by Coca Cola Co., Ltd.

* Corresponding author. Tel./fax: +86 551 2901450.

E-mail address: wentaohao@ustc.edu (W. Hao).

We chose recycled PET materials from drinking water bottles for two reasons: 1) they are easily collected; 2) it is of high practical value to study the influence of nanoparticles on the non-isothermal crystallization kinetics of recycled PET. Si_3N_4 nanoparticles were purchased from Hefei Kaier Nanometer Energy & technology Co., Ltd. (China). According to the technological documents accompanying the products, the diameter of the nanoparticles is not more than 20 nm. Silicane coupling agent with aminogroup, KH-550, was purchased from Nanjing Capatue Chemical Co., Ltd. (China).

2.2. Equipments and instruments

The twin-screw internal mixer, model XSS-300, is manufactured by Shanghai Kechuang Rubber Plastic Mechanical Equipment Co., Ltd., China. Pyris Diamond differential scanning calorimeter is a product of Perkin Elmer Inc., USA.

2.3. Sample preparation

Before being incorporated into PET, the Si_3N_4 nanoparticles were treated with the coupling agent. After the PET fragments were completely melted, the Si_3N_4 nanoparticles were mixed into the melt and blended for another 5 min. Samples for DSC measurement were cut from the cooled down composites. All the samples are termed as PET-X, where X refers to the Si_3N_4 content. For example, the sample PET-1 refers to the PET- Si_3N_4 nanocomposite with Si_3N_4 contents of 1 wt%.

2.4. DSC measurement

For every DSC run, a piece of PET- Si_3N_4 nanocomposite of about 8 mg was put into the DSC pan and carefully sealed. The samples were first heated to 270 °C, held for 5 min and then were cooled at a constant rate to 50 °C. The preset cooling rates were 5, 10, 20 and 40 °C/min respectively.

3. Results and discussion

3.1. The non-isothermal crystallization processes

The crystallization exotherms of PET and PET-1 are shown in Fig. 1. It can be seen that the exothermic peaks of original PET are sharper and the peak temperatures are higher compared with those shown in the literature [20,21]. This indicates that the crystallization rate of the recycled PET is faster than that of the in-situ polymerized materials. However, it is surprising that the crystallization peaks of PET-1 are even sharper than the original PET, and the peak heights are also greater (see Fig. 1(b)). This is evidence that 1 wt% Si_3N_4 nanoparticles have a strong accelerating effect on crystallization of PET.

However, it is totally different when more Si_3N_4 nanoparticles were added into PET. As shown in Fig. 2, the exothermic peaks of sample PET-2 shift to lower temperatures and the peak shape also changes greatly. Although the peak crystallization temperatures of sample PET-3 and PET-

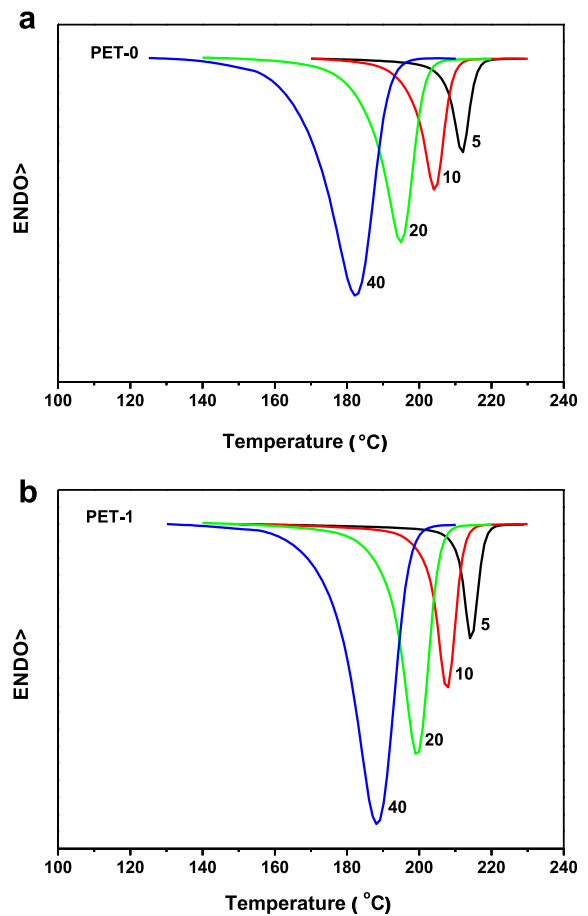


Fig. 1. DSC diagrams of PET (a) and PET- Si_3N_4 (1 wt%) nanocomposites (b).

4 are higher than that of PET-2, they are still less than or almost equal to that of the original PET. It seems that the crystallization of PET is hindered by Si_3N_4 nanoparticles when the loading is higher than 1 wt%.

Non-isothermal crystallization data for PET and all the nanocomposites are collected in Table 1. Clearly, the peak

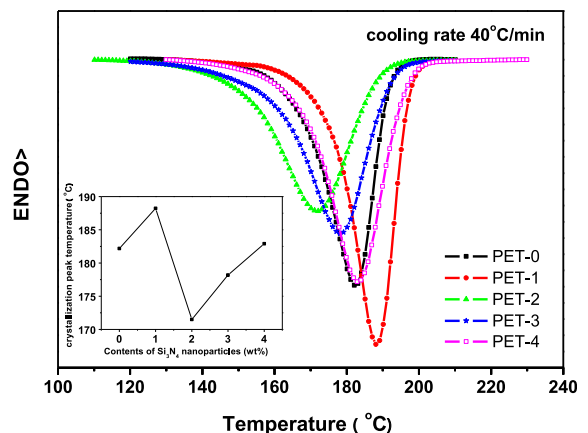


Fig. 2. DSC diagrams of PET- Si_3N_4 nanocomposites (cooling rate, 40 °C/min).

Table 1

Non-isothermal crystallization data of PET and PET-Si₃N₄ nanocomposites during cooling process.

Cooling rate (°C/min)	5		10		20		40	
	T _p ^a (°C)	ΔT ₁ ^b (°C)	T _p (°C)	ΔT ₁ (°C)	T _p (°C)	ΔT ₁ (°C)	T _p (°C)	ΔT ₁ (°C)
PET-0	211.80	5.11	204.20	6.71	194.72	9.58	182.18	14.04
PET-1	214.32	4.47	207.57	6.07	199.43	8.62	188.23	13.09
PET-2	208.46	7.35	199.37	10.53	187.72	14.37	171.51	21.71
PET-3	211.41	7.35	203.05	10.21	192.40	14.05	178.19	18.84
PET-4	213.41	6.38	205.91	8.94	196.10	11.81	182.90	16.6

^a T_p – the peak crystallization temperature.

^b ΔT₁ – the half peak width.

temperature T_p value is highest when the Si₃N₄ content is 1 wt% and reduces as the particle content increases to 2–4 wt%. The half peak width ΔT₁ can also be used to characterize the crystallization rate of polymer materials. As shown in Table 1, the ΔT₁ value is smallest when the Si₃N₄ content is 1 wt%, while when the Si₃N₄ content is more than 1 wt%, the ΔT₁ values are higher than that of original PET. Apparently, the crystallization rate of the composites is slower than the original PET when the Si₃N₄ content is 2–4 wt%.

Initial crystallization temperature (T_i) is an important parameter in characterization of the nucleation effect of the nanoparticles on the polymer composites [22]. The extrapolated T_is are shown in Table 2. Clearly, the extrapolated T_is of the PET-Si₃N₄ nanocomposites are almost all higher than or equal to that of the original PET. That is, the Si₃N₄ nanoparticles have a good nucleation effect on the crystallization of PET within the content range studied. This seems to be contrary to the fact that the total crystallization rate of PET is slower than the original PET when the Si₃N₄ loading is more than 1 wt%. The only possibility is that the crystal growth rate of PET is slower. The movement of PET segments is restricted to some degree by the Si₃N₄ nanoparticles.

3.2. Application of Avrami and Mo methods

Avrami and Mo methods are always applied in analyzing the non-isothermal crystallization of polymer materials. It was proposed by Avrami [23,24] that the relationship between the relative crystallinity (X_t) and the crystallization time (t) could be described as follows,

$$1 - X_t = \exp(-kt^n) \quad (1)$$

Or,

Table 2

Initial crystallization temperatures of PET and PET-Si₃N₄ nanocomposites.

T _i (°C)	Cooling rate (°C/min)				Extrapolated T _i (°C)
	5	10	20	40	
PET-0	215.74	209.25	201.45	191.51	216.90
PET-1	218.00	212.28	205.49	197.17	218.88
PET-2	214.72	207.95	199.24	188.39	216.13
PET-3	216.77	210.47	202.47	191.92	218.21
PET-4	218.72	212.97	205.69	195.97	220.06

$$\ln[-\ln(1 - X_t)] = n \ln t + \ln k \quad (2)$$

where X_t can be determined by Formula (3), in which dH/dt refers to the time-dependent enthalpy change during the non-isothermal crystallization.

$$X(t) = \int_0^t (dH/dt) dt / \int_0^\infty (dH/dt) dt \quad (3)$$

Fig. 3 is the variation of the relative crystallinity with the crystallization time for PET and PET-1. Fig. 4 presents the plots of ln[-ln(1-X_t)] versus ln t of the same samples according to Equation (2). The kinetic parameters for all the PET samples are listed in Table 3, in which the Z_c value is the modified cooling rate constant proposed by Jeziorny [25], ln Z_c = (ln k)/β.

As shown in Table 3, the half crystallization time t_{1/2} of sample PET-1 is shorter than that of the original PET, indicating that the crystallization of PET is accelerated by 1 wt% Si₃N₄ nanoparticles. However, it can also be clearly seen from Fig. 3 that the crystal growth process is prolonged and the total crystallization time of the 1 wt% sample is much longer than that of the original PET.

After treatment with silane coupling agent KH-550, the Si₃N₄ nanoparticles are coated with amino groups which may react with the PET molecules and result in strong interaction between the particles and the PET segments.

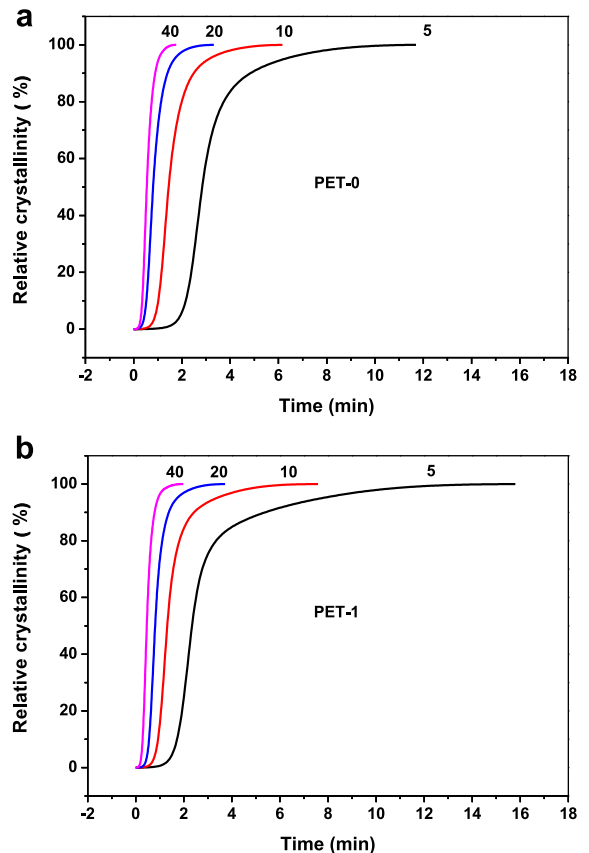


Fig. 3. Variation of relative crystallinity to crystallization time of PET (a) and PET-Si₃N₄ (1 wt%) nanocomposites (b).

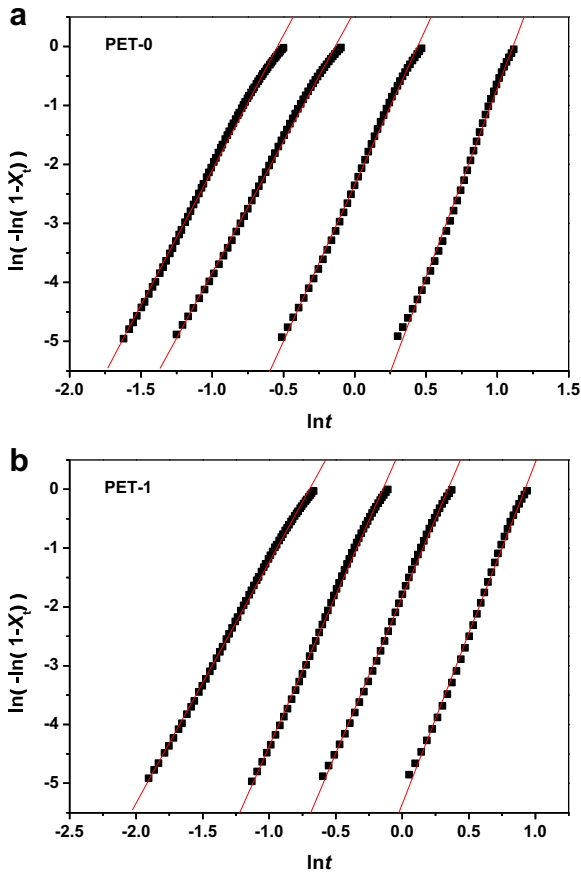


Fig. 4. Plots of $\ln[-\ln(1-X_t)]-\ln t$ of PET (a) and PET-Si₃N₄ (1 wt%) nanocomposites.

Consequently, the movement of PET molecules is effectively restricted. Although the large surface to volume ratio of Si₃N₄ nanoparticles favors the nucleation process of PET, the interaction functions negatively. The net effect is that

Table 3
Parameters obtained from the Avrami Analysis.

Sample	β (K/min)	n	Z_c	$t_{1/2}$ (min)
PET-0	5	6.74	0.23	2.85
	10	5.38	0.62	1.44
	20	4.45	1.13	0.80
	40	4.52	1.63	0.54
PET-1	5	6.01	0.33	2.34
	10	5.41	0.69	1.32
	20	5.11	1.16	0.81
	40	4.08	1.77	0.46
PET-2	5	5.26	0.30	2.95
	10	4.82	0.53	1.81
	20	4.10	0.88	1.08
	40	3.77	1.17	0.74
PET-3	5	4.60	0.42	2.38
	10	5.05	0.52	1.78
	20	3.88	0.95	0.98
	40	4.08	1.26	0.69
PET-4	5	4.57	0.43	2.32
	10	4.72	0.62	1.55
	20	4.46	0.95	0.98
	40	3.81	1.38	0.60

the crystallization rate decreases. Similar results can also be found in the literature [26–28].

From Table 3, it can be seen that the Avrami index n values are larger than that of in-situ polymerized PET nanocomposites [29,30], but some researchers have also reported similar values ($n > 4$) for commercial PET [31,32]. Apparently, the n value decreases with the Si₃N₄ content which indicates that Si₃N₄ nanoparticles can function as good heterogeneous nucleating agents for PET like other nano-sized fillers [33].

The Mo method is the combination of Avrami and Ozawa equations [34], and the simplified formula is:

$$\ln \beta = \ln F(T) - a \ln t \tag{4}$$

where $F(T)$ refers to the value of the cooling rate chosen at a unit crystallization time at which the system has a certain degree of crystallinity.

According to Equation (4), straight lines with intercept of $\ln F(T)$ and slope a can be obtained by plotting $\ln \beta$ versus $\ln t$ (see Fig. 5). Data of $\ln F(T)$ and a are collected in Table 4. It can be seen that the $F(T)$ value is the lowest when the Si₃N₄ content is 1 wt%, while it has higher values when the Si₃N₄ content is more than 1 wt%. Such results are similar to those obtained in the analysis on the half peak width ΔT_1 (as shown in Table 1).

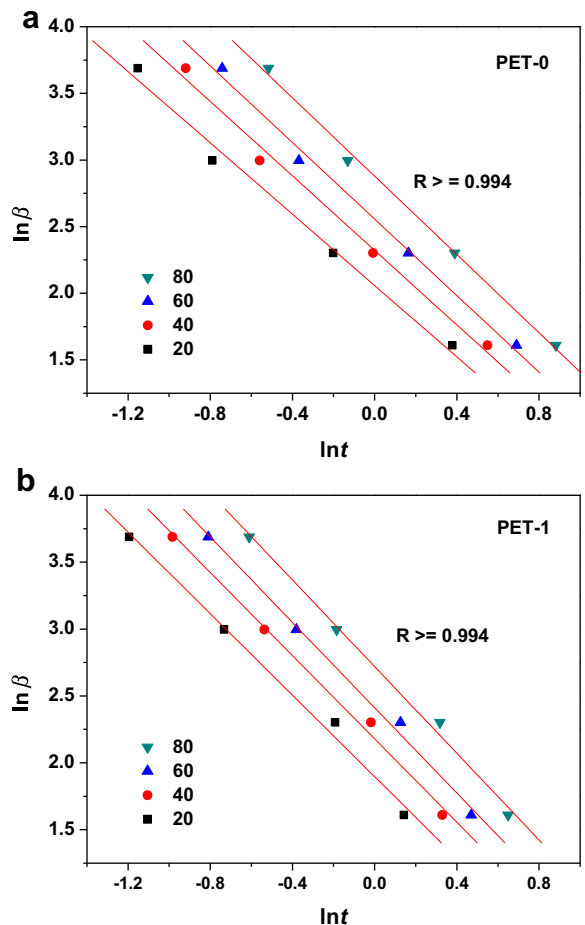


Fig. 5. The Mo plots of PET (a) and PET-Si₃N₄ (1 wt%) nanocomposite (b).

Table 4
Parameters of non-isothermal crystallization kinetics from Mo analysis.

Samples		Relative Crystallinity (%)			
		20	40	60	80
PET-0	$F(T)$	7.85	10.18	12.94	17.81
	a	1.38	2.32	2.56	2.88
PET-1	$F(T)$	6.62	8.85	11.25	15.18
	a	1.90	2.18	2.41	2.72
PET-2	$F(T)$	11.94	17.12	23.10	32.46
	a	2.48	2.85	3.14	3.48
PET-3	$F(T)$	11.13	15.64	21.33	31.82
	a	2.41	2.75	3.05	3.46
PET-4	$F(T)$	9.49	13.46	17.81	25.28
	a	2.25	2.59	2.87	3.22

3.3. Activation energy of PET-Si₃N₄ nanocomposites during crystallization

Detailed kinetic analysis will provide us with more information about the thermal transition inside the polymer materials. The Kissinger method [35] is perhaps the most commonly used, through which the activation energy of the non-isothermal crystallization process can be easily obtained [32,36]. Furthermore, the crystallinity dependence of the activation energy can be determined [37] by applying the Flynn-Wall-Ozawa equation [38,39].

The basic form of the Kissinger equation is shown in formula (5), where β_i is the cooling rate, T_p is the peak temperature, E is the activation energy and R is the gas constant.

$$\ln\left(\frac{\beta_i}{T_p^2}\right) = \text{const.} - \frac{E}{RT_{p,i}} \quad (5)$$

Straight lines with correlation coefficient more than 0.990 were obtained by plotting $\ln(\beta/T_p^2)$ versus $1/T_p$. The Kissinger activation energy E for PET-Si₃N₄ nanocomposites with different particle contents was calculated from the slopes of the straight lines and results are shown in Fig. 6. It is apparent that the activation energy of sample PET-1 is the lowest and the E values for the other composites are all higher than the original PET.

Generally, the Kissinger activation energy characterizes the difficulty of the crystallization process. It is apparent that 1 wt% Si₃N₄ nanoparticles can accelerate the crystallization of PET, while higher loading particles hinder the crystallization.

By substituting the peak temperature (T_p) in the original Kissinger equation to initial crystallization temperature (T_i), the activation energy related to the nucleation process (E_N) can also be determined [19]. The results are shown in Fig. 7. Clearly, the E_N value of sample PET-1 is the lowest,

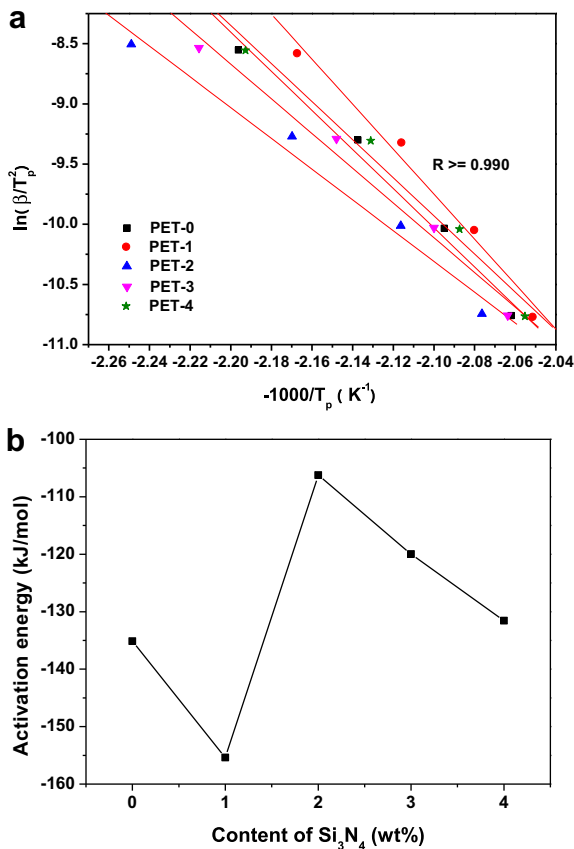


Fig. 6. Kissinger activation energy of PET-Si₃N₄ nanocomposites derived from the PEAK crystallization temperature.

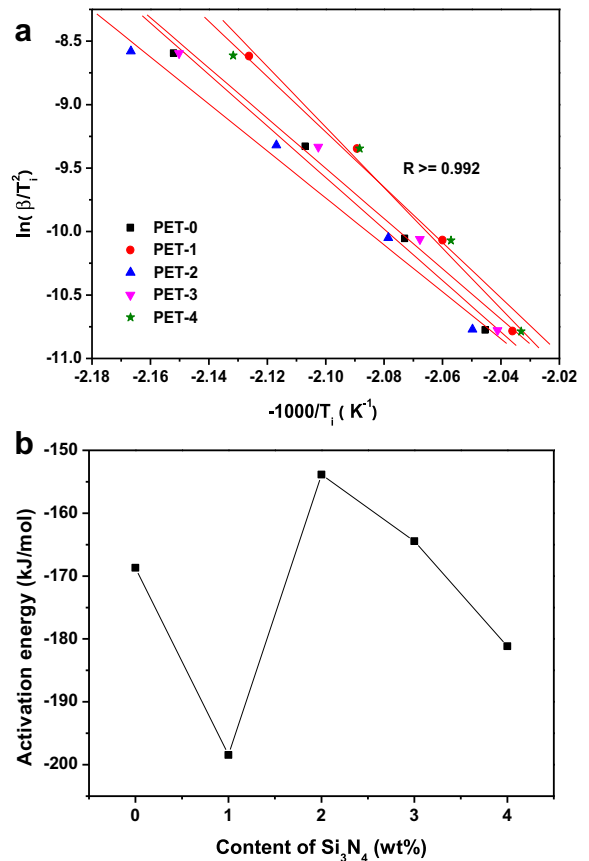


Fig. 7. Kissinger activation energy of PET-Si₃N₄ nanocomposites derived from the INITIAL crystallization temperature.

indicating the excellent nucleation effect of Si_3N_4 nanoparticles at a concentration of 1 wt%. For the sample PET-4, the E_N value is lower than that of original PET, but the E value of PET-4 is higher than that of the original PET. This also indicates that Si_3N_4 nanoparticles have a good nucleation effect and are a hindrance to crystal growth of Si_3N_4 nanoparticles.

Because of its relative conciseness and accuracy, the isoconversional method of Flynn-Wall-Ozawa (FWO) is always applied in treatment of chemical or physical processes with temperature change [40], including cross-linking [41] and crystallization [31]. The basic form of FWO equation is shown as following,

$$\ln(\beta_i) = \text{Const.} - \frac{1.05E_\alpha}{RT_{\alpha,i}} \quad (6)$$

where β_i represents the cooling rate, E_α stands for activation energy at a certain conversion, R is the gas constant and $T_{\alpha,i}$ is the temperature at certain conversions and cooling rate.

The plots of $\ln\beta_i$ vs. $1/T_{\alpha,i}$ of sample PET and PET-1 are shown in Fig. 8, and the activation energy E_α of all the PET- Si_3N_4 nanocomposites calculated from the slope of the lines

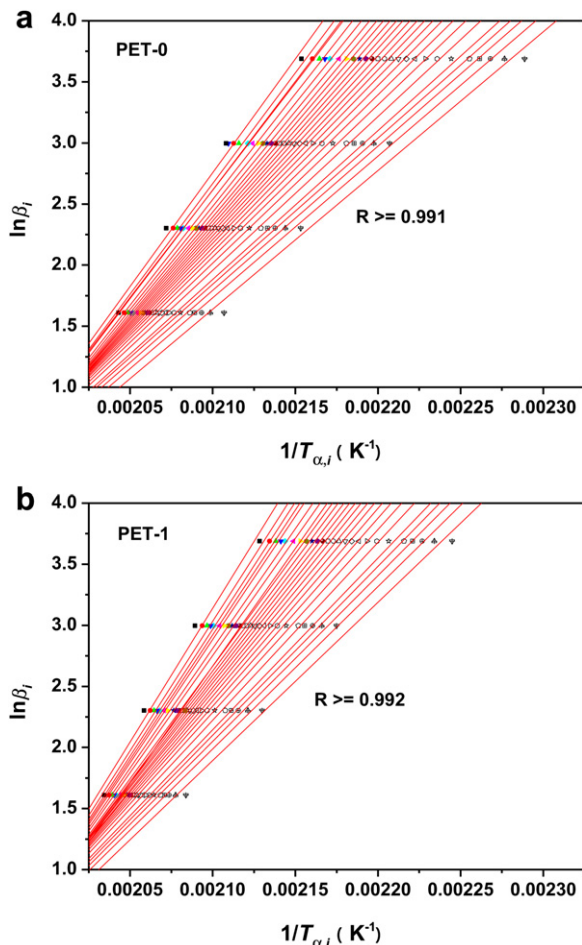


Fig. 8. Plots of $\ln\beta_i$ vs. $1/T_{\alpha,i}$ of PET (a) and PET- Si_3N_4 (1 wt%) nanocomposites (b).

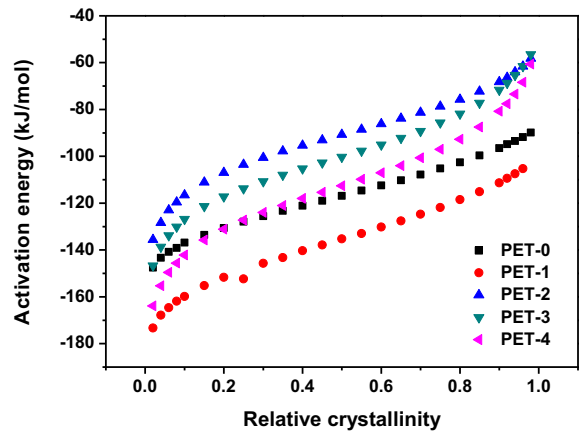


Fig. 9. Flynn-Wall-Ozawa activation energy of the PET- Si_3N_4 nanocomposites.

are shown in Fig. 9. It can be seen that the E_α value increases constantly with the relative crystallinity, suggesting that the movement of the segments of PET is more and more restricted as the relative crystallinity increases, while the temperature reduces [21].

Apparently, the E_α value of sample PET-1 is the lowest, while it is highest for PET-2. Such results agree well with the Kissinger analysis. For sample PET-4, the E_α value is smaller than that of the original PET at low crystallinity (<20%). It also indicates that the Si_3N_4 nanoparticles have a good nucleation effect. However, the activation energy becomes larger than that of the original PET at higher crystallinity. This can also be attributed to the interaction among the nanoparticles and the PET molecules, which strongly restricts the movement of the PET segments.

4. Conclusions

From the analysis of the non-isothermal crystallization kinetics of PET- Si_3N_4 nanocomposites, it can be concluded that Si_3N_4 nanoparticles have a good nucleation effect on crystallization of PET. However, the crystal growth of PET is slowed down by the Si_3N_4 nanoparticles. Possibly, this is due to the interaction between surface treated Si_3N_4 nanoparticles and the PET segments. Results obtained from activation energy analysis agree well with those obtained in general analysis on the non-isothermal crystallization, which are also supported by Avrami analysis and Mo treatment.

Acknowledgements

Thanks to the Natural Science Funding of Anhui Province (2010AKZR0829) and the Key projects of Scientific Research of Anhui Educational Department (2011AJZR0922).

References

- [1] F. Welle, Twenty years of PET bottle to bottle recycling—an overview, *Resour. Conserv. Recy.* (2011). doi:10.1016/j.resconrec.2011.04.009.
- [2] P. Esena, S. Zanini, C. Riccardi, Plasma processing for surface optical modifications of PET films, *Vacuum* 82 (2008) 232–235.

- [3] H.J. Bang, H.Y. Kim, F.L. Jin, S.J. Park, Fibers spun from 1,4-cyclohexane-dimethanol-modified polyethylene terephthalate resin, *J. Ind. Eng. Chem.* (2011). doi:10.1016/j.jiec.2011.05.021.
- [4] M.T.M. Bizarria, A.L.F. de M. Giraldo, C.M. de Carvalho, J.I. Velasco, M. A. d'Ávila, L.H.I. Mei, Morphology and thermomechanical properties of recycled PET-organoclay nanocomposites, *J. Appl. Polym. Sci.* 104 (2007) 1839–1844.
- [5] G. Wang, Y. Chen, Q. Wang, Structure and properties of poly(ethylene terephthalate)/Na⁺-montmorillonite nanocomposites prepared by solid state shear milling (S²M) method, *J. Polym. Sci., Part B Polym. Phys.* 46 (2008) 807–817.
- [6] C.I.W. Calcagno, C.M. Mariani, S.R. Teixeira, R.S. Mauler, The effect of organic modifier of the clay on morphology and crystallization properties of PET nanocomposites, *Polymer* 48 (2007) 966–974.
- [7] S.J. Lee, W.G. Hahm, T. Kikutani, B.C. Kim, Effects of clay and POSS nanoparticles on the quiescent and shear-induced crystallization behavior of high molecular weight poly(ethylene terephthalate), *Polym. Eng. Sci.* 49 (2008) 317–323.
- [8] Y. Wang, J. Gao, Y. Ma, U.S. Agarwal, Study on mechanical properties, thermal stability and crystallization behavior of PET/MMT nanocomposites, *Composites Part B* 37 (2006) 399–407.
- [9] H. Zheng, J. Wu, Preparation, crystallization, and spinnability of poly(ethylene terephthalate)/silica nanocomposites, *J. Appl. Polym. Sci.* 103 (2007) 2564–2568.
- [10] Q. Ji, X. Wang, Y. Zhang, Q. Kong, Y. Xia, Characterization of poly(ethylene terephthalate)/SiO₂ nanocomposites prepared by sol-gel method, *Composites Part A* 40 (2009) 878–882.
- [11] Y. Ke, T. Wu, Y. Xia, The nucleation, crystallization and dispersion behavior of PET-monomodisperse SiO₂ composites, *Polymer* 48 (2007) 3324–3336.
- [12] C. Ge, P. Ding, L. Shi, J. Fu, Isothermal crystallization kinetics and melting behavior of poly(ethylene terephthalate)/barite nanocomposites, *J. Polym. Sci., Part B Polym. Phys.* 47 (2009) 655–668.
- [13] W. Gao, B. Zhou, X. Ma, Y. Liu, Z. Wang, Y. Zhu, Preparation and characterization of BaSO₄/poly(ethylene terephthalate) nanocomposites, *Colloids Surf. A* 385 (2011) 181–187.
- [14] M. Xanthos, B.C. Baltzis, P.P. Hsu, Effects of carbonate salts on crystallization kinetics and properties of recycled poly(ethylene terephthalate), *J. Appl. Polym. Sci.* 64 (1997) 1423–1435.
- [15] F.L. Riley, Silicon nitride and related materials, *J. Am. Ceram. Soc.* 83 (2000) 245–265.
- [16] W. Zhou, C. Wang, T. Ai, K. Wu, F. Zhao, H. Gu, A novel fiber-reinforced polyethylene composite with added silicon nitride particles for enhanced thermal conductivity, *Comp. Part A* 40 (2009) 830–836.
- [17] Y. Tai, J. Miao, J. Qian, R. Xia, Y. Zhang, An effective way to stabilize silicon nitride nanoparticles dispersed in rubber matrix by a one-step process, *Mater. Chem. Phys.* 112 (2008) 659–667.
- [18] W. Hao, W. Yang, H. Cai, Y. Huang, Non-isothermal crystallization kinetics of polypropylene/silicon nitride nanocomposites, *Polym. Test* 29 (2010) 527–533.
- [19] W. Hao, W. Li, W. Yang, L. Shen, Effect of silicon nitride nanoparticles on the crystallization behavior of polypropylene, *Polym. Test* 30 (2011) 527–533.
- [20] G. Antoniadis, K.M. Paraskevopoulos, A.A. Vassiliou, G.Z. Papa-georgioub, D. Bikiaris, K. Chrissafis, Nonisothermal melt-crystallization kinetics for in situ prepared poly(ethylene terephthalate)/monmorillonite (PET/OMMT), *Thermochim. Acta* 521 (2011) 161–169.
- [21] G. Antoniadis, K.M. Paraskevopoulos, D. Bikiaris, K. Chrissafis, Non-isothermal crystallization kinetic of poly(ethylene terephthalate)/fumed silica (PET/SiO₂) prepared by in situ polymerization, *Thermochim. Acta* 510 (2010) 103–112.
- [22] P. Bhimaraj, H. Yang, R.W. Siegel, L.S. Schadler, Crystal nucleation and growth in poly(ethylene terephthalate)/alumina-nanoparticle composites, *J. Appl. Polym. Sci.* 106 (2007) 4233–4240.
- [23] M. Avrami, Kinetics of phase change. I General theory, *J. Chem. Phys.* 7 (1939) 1103–1112.
- [24] M. Avrami, Kinetics of phase change. II transformation-time relations for random distribution of nuclei, *J. Chem. Phys.* 8 (1940) 212–224.
- [25] A. Jeziorny, Parameters characterizing the kinetics of the non-isothermal crystallization of poly(ethylene terephthalate) determined by DSC, *Polymer* 19 (1978) 1142–1144.
- [26] D. Wu, C. Zhou, X. Fan, D. Mao, Z. Bian, Nonisothermal crystallization kinetics of poly(butylene terephthalate)/montmorillonite nanocomposites, *J. Appl. Polym. Sci.* 99 (2006) 3257–3265.
- [27] C.F. Ou, M.T. Ho, J.R. Lin, Synthesis and characterization of poly(ethylene terephthalate) nanocomposites with organoclay, *J. Appl. Polym. Sci.* 91 (2004) 140–145.
- [28] V.D. Deshpande, S. Jape, Nonisothermal crystallization kinetics of nucleated poly(ethylene terephthalate), *J. Appl. Polym. Sci.* 111 (2009) 1318–1327.
- [29] X. Chen, C. Li, W. Shao, T. Liu, L. Wang, Nonisothermal crystallization kinetics of poly(ethylene terephthalate)/antimony-doped tin oxide nanocomposites, *J. Appl. Polym. Sci.* 109 (2008) 3753–3762.
- [30] S.Y. Hwang, W.D. Lee, J.S. Lim, K.H. Park, S.S. IM, Dispersibility of clay and crystallization kinetics for in situ polymerized PET/pristine and modified montmorillonite nanocomposites, *J. Polym. Sci. Part B Polym. Phys.* 46 (2008) 1022–1035.
- [31] G. Antoniadis, K.M. Paraskevopoulos, D. Bikiaris, K. Chrissafis, Melt-crystallization mechanism of poly(ethylene terephthalate)/multi-walled carbon nanotubes prepared by in situ polymerization, *J. Polym. Sci. Part B Polym. Phys.* 47 (2009) 1452–1466.
- [32] Y. Wang, C. Shen, H. Li, Q. Li, J. Chen, Nonisothermal melt crystallization kinetics of poly(ethylene terephthalate)/clay nanocomposites, *J. Appl. Polym. Sci.* 91 (2004) 308–314.
- [33] G. Hu, X. Feng, S. Zhang, M. Yang, Crystallization behavior of poly(ethylene terephthalate)/multiwalled carbon nanotubes composites, *J. Appl. Polym. Sci.* 108 (2008) 4080–4089.
- [34] T. Liu, Z. Mo, S. Wang, H. Zhang, Nonisothermal melt and cold crystallization kinetics of poly(aryl ether ether ketone ketone), *Polym. Eng. Sci.* 37 (1997) 568–575.
- [35] H.E. Kissinger, Variation of peak temperature with heating rate in differential thermal analysis, *J. Res. Natl. Bur. Stand* 57 (1956) 217.
- [36] C. Ge, L. Shi, H. Yang, S. Tang, Nonisothermal melt crystallization kinetics of poly(ethylene terephthalate)/barite nanocomposites, *Polym. Compos.* 31 (2010) 1504–1514.
- [37] G. Papageorgiou, D.N. Bikiarisa, K. Chrissafis, A different approach for the study of the crystallization kinetics in polymers. Key study: poly(ethylene terephthalate)/SiO₂ nanocomposites, *Polym. Int.* 59 (2010) 1630–1638.
- [38] J.H. Flynn, L.A. Wall, General treatment of the thermogravimetry of polymers, *J. Res. Natl. Bur. Stand* 70A (1966) 487–523.
- [39] T. Ozawa, A new method of analyzing thermogravimetric data, *Bull. Chem. Soc. Jpn.* 38 (1965) 1881–1886.
- [40] S. Vyazovkin, N. Sbirrazzuoli, Isoconversional kinetic analysis of thermally stimulated processes in polymers, *Macromol. Rapid Commun.* 27 (2006) 1515–1532.
- [41] W. Hao, J. Hu, L. Chen, J. Zhang, L. Xing, W. Yang, Isoconversional analysis of non-isothermal curing process of epoxy resin/epoxide polyhedral oligomeric silsesquioxane composites, *Polym. Test* 30 (2011) 349–355.